Prestin's Anion Transport and Voltage-Sensing Capabilities Are Independent

Jun-Ping Bai,[†] Alexei Surguchev,[†‡] Simone Montoya,[†‡] Peter S. Aronson,[§¶] Joseph Santos-Sacchi,[‡¶‖] and Dhasakumar Navaratnam[†‖*]

[†]Department of Neurology, [‡]Division of Otolaryngology, Department of Surgery, [§]Department of Internal Medicine, [¶]Department of Cellular and Molecular Physiology, and [‖]Department of Neurobiology, Yale University School of Medicine, New Haven, Connecticut

ABSTRACT The integral membrane protein prestin, a member of the SLC26 anion transporter family, is responsible for the voltage-driven electromotility of mammalian outer hair cells. It was argued that the evolution of prestin's motor function required a loss of the protein's transport capabilities. Instead, it was proposed that prestin manages only an abortive hemicycle that results in the trapped anion acting as a voltage sensor, to generate the motor's signature gating charge movement or nonlinear capacitance. We demonstrate, using classical radioactive anion ([^{14}C]formate and [^{14}C]oxalate) uptake studies, that in contrast to previous observations, prestin is able to transport anions. The prestin-dependent uptake of both these anions was twofold that of cells transfected with vector alone, and comparable to SLC26a6, prestin's closest phylogenetic relative. Furthermore, we identify a potential chloride-binding site in which the mutations of two residues (P328A and L326A) preserve nonlinear capacitance, yet negate anion transport. Finally, we distinguish 12 charged residues out of 22, residing within prestin's transmembrane regions, that contribute to unitary charge movement, i.e., voltage sensing. These data redefine our mechanistic concept of prestin.

INTRODUCTION

It is now well established that prestin drives voltage-dependent electromotility in mammalian outer hair cells (1–4). Although its primary sequence places it in the SLC26 family of anion transporters, two early findings suggested that prestin (SLC26a5) was different from other members of this family. First, prestin uniquely imparts voltage-dependent mechanical activity and its corresponding electrical signature, gating charge movements, or nonlinear capacitance (NLC) (1,2). Second, unlike its nonmammalian orthologs and mammalian family members, prestin reportedly cannot transport anions (6,7). An attempt to discover how prestin senses voltage led to mutation analyses of 21 charged residues found in prestin that are not conserved in SLC26a6, its closest phylogenetic-related protein that lacks NLC (8). Such mutations failed to alter the Boltzmann parameter that corresponds to a voltage-evoked unitary gating charge (α or z). These observations led Oliver et al. (8) to invoke an incomplete transport cycle (with a hemimovement of anions within the intramembranous protein) as the mechanism by which prestin achieves its voltage sensitivity, thereby underlying the generation of NLC (8). This is generally known as the extrinsic voltage sensor or partial anion transporter hypothesis. Evidence was presented against this hypothesis, and in favor of the argument that anions work allosterically, by modifying the energy profile of the intramembranous motor protein, prestin (9–11).

Here we test key premises underlying the extrinsic voltage sensor hypothesis, i.e., that prestin is not an anion transporter, and that prestin lacks an intrinsic voltage sensor. We show that: 1), prestin transports anions; 2), intrinsic charged residues contribute to voltage sensing; and 3), by mutation, these two functions of prestin can be divorced. These observations, in conjunction with others (9,10,12), cast doubt on a simple extrinsic voltage-sensing scheme.

METHODS

The assumption that mammalian prestin is unable to transport anions is based, in part, on a reported failure of anion transport in oocytes (7), involving data that we have replicated (J.-P. Bai and D. Navaratnam, unpublished observations). Therefore, we chose to use heterologous expression in Chinese hamster ovary (CHO) cells to evaluate prestin's ability to transport [^{14}C]formate and [^{14}C]oxalate. CHO cells were used extensively to characterize prestin's NLC.

We fused YFP (in eYFPN1, Clontech, Mountain View, CA) to the C-terminus of prestin (including all mutants), as previously described (13). This step allowed us to verify that transfection efficiency was comparable, and to identify cells transfected with prestin for electrophysiological recording. We expressed murine SLC26a6 (14) in pcDNA 3.1, which contains the identical cytomegalovirus promoter. We mutated individual residues using the Quikchange mutagenesis kit (Stratagene, La Jolla, CA). Mutagenesis was confirmed by sequencing the entire transcript.

Each transport experiment was performed using a 24-well plate (Costar/Corning, Lowell, MA). Cells were plated at a concentration of 200,000 cells per well, and transfected with lipofectamine 24 h after plating (as previously described) (13). Each experimental variable was evaluated in triplicate wells. Each experiment included three wells transfected with empty vector (negative control), and three wells transfected with prestin (positive control) to control for experimental variables (e.g., transfection/plating efficiency). We used 0.8 μg of DNA and 1.6 μL of lipofectamine per well. Formate or oxalate uptake was assayed 24 h after transfection. Cells were incubated with 120 mM NaCl, 20 mM HEPES, 5 mM KCl, 5 mM glucose, 2 mM $CaCl_2$, and 1 mM $MgCl_2$ (pH 7.4) for 30 min. After aspiration of the NaCl solution, cells were incubated in 130 mM K gluconate, 20 mM HEPES, and 5 mM glucose (pH 7.4), containing 20 μM of [^{14}C]formate

Submitted September 26, 2008, and accepted for publication December 23, 2008.

*Correspondence: dhasakumar.navaratnam@yale.edu

Editor: Tzyh-Chang Hwang.

© 2009 by the Biophysical Society

0006-3495/09/04/3179/8 $2.00

doi: 10.1016/j.bpj.2008.12.3948

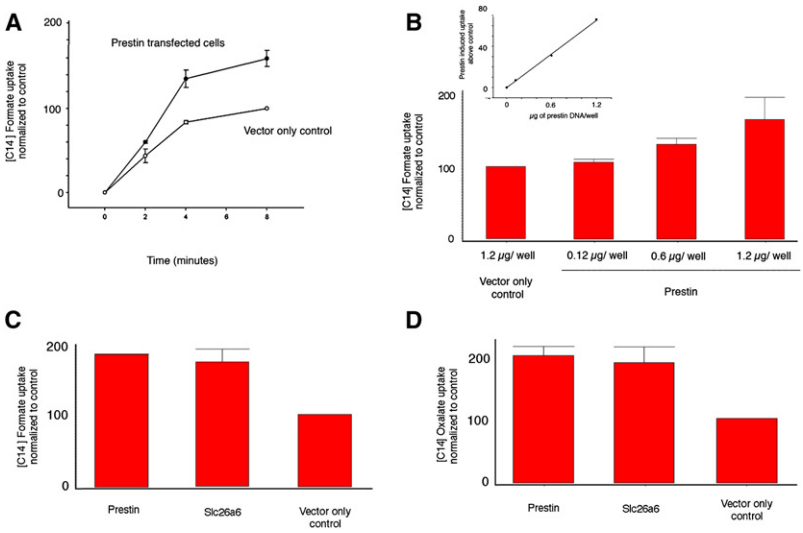

FIGURE 1 Prestin-transfected CHO cells indicate anion transport. (*A*) CHO cells transfected with prestin show a time-dependent uptake of [^{14}C]formate that was greater than that of CHO cells transfected with empty vector alone (control). Uptake of [^{14}C]formate by prestin-transfected cells at 2, 4, and 8 min was 60 (±8.2), 135 (±10.4), and 160 (±9.5), respectively. In contrast, the uptake of control cells at corresponding time points was 44 (±8.2), 84 (±2.2) and 100 ($n = 3$). Data were normalized to vector-only controls at 8 min, which was given a value of 100. (*B*) There is a dose-dependent increase in [^{14}C]formate uptake in cells transfected with increasing quantities of prestin-YFP plasmid. The mean uptake for cells transfected with 0.12 μg, 0.6 μg, and 1.2 μg of prestin plasmid DNA were 107 (±4), 131 (±8.5), and 166 (±31), respectively. Control wells were transfected with 1.2 μg of YFP plasmid DNA ($n = 3$). (*Inset*) Linear relationship between transport induced by prestin (after subtracting background) and amount of DNA used in transfection. (*C* and *D*) CHO cells transfected with prestin and Slc26a6 show increased uptake of [^{14}C]formate (*C*) and [^{14}C]oxalate (*D*) compared with control (YFP vector only). The plot shows mean uptake per 200,000 cells contained in a well (of a 24-well plate) ± SE. Data were normalized to vector-only controls ($n = 3$, in each case). Controls were assigned a value of 100. The uptake of [^{14}C]formate by prestin and Slc26a6 was 183 (±0.7) and 171 (±17.3), respectively, i.e., significantly different from controls ($p < 0.01$, one-way ANOVA). The uptake of [^{14}C]oxalate by prestin and Slc26a6 was 198 (±13.5) and 187 (±24.0), respectively, i.e., significantly different from vector-only controls ($p < 0.05$, one-way ANOVA). The absolute prestin-induced uptake of oxalate was 1.5-fold greater than formate uptake; this was obscured by normalization. Uptake is denoted in relative counts (see Methods).

(or [^{14}C]oxalate) for 8 min (in the standard assay, or at other time points indicated in timed experiments). Cells were washed three times with ice-cold 130 mM K gluconate, 20 mM HEPES, and 5 mM glucose. Cells were then lysed with 0.2 mL of 0.5 M NaOH, neutralized with 0.5 M HCl, and [^{14}C]formate (or [^{14}C]oxalate) uptake was determined by liquid scintillation counting. All data are reported as [^{14}C]formate (or [^{14}C]oxalate) uptake per 200,000 cells, and are mean values from 3–4 experiments (±SE) that were normalized to vector-only controls. Thus, uptake in the figures is denoted in relative counts. Each experiment, in turn, represents the mean of triplicate wells. The absolute mean uptake of [^{14}C]formate and [^{14}C]oxalate in a given control well across a number of experiments was ~20 pmol and 28 pmol per 200,000 cells, respectively. In independent experiments, we established by both protein and DNA assays that transfection with different plasmids did not affect the cell number within the first 24 h. Knowing the intracellular concentration of transported anions would be important in evaluating the actual fluxes that may occur in vivo. We are aware of no data concerning intracellular concentrations of oxalate or formate, or methods for their measurement. Fortunately, we are simply making a determination here that anion transport occurs, and this determination is independent of intracellular concentrations. Confocal microscopy was performed as previously described, using YFP fusions of each mutant (13).

Whole-cell patch clamp recordings were performed at room temperature, using an Axon 200B amplifier (Axon Instruments, Union City, CA), as described previously (13). Cells were recorded 48 h after transfection, to allow for stable measurements of nonlinear capacitance. Ionic blocking solutions were used to isolate capacitive currents. The bath solution contained (in mM): TEA 20, CsCl 20, $CoCl_2$ 2, $MgCl_2$ 1.47, HEPES 10, NaCl 99.2, and $CaCl_2 \cdot 2H_2O$ 2, pH 7.2, and the pipette solution contained (in mM): CsCl 140, EGTA 10, $MgCl_2$ 2, and HEPES 10, pH 7.2. Osmolarity was adjusted to 300 ± 2 mOsm with dextrose. Command delivery and data collections were performed with a Windows-based whole-cell voltage-clamp program, jClamp (Scisoft, New Haven, CT), using an NI PCI 6052E interface (National Instruments). We corrected for the effects of series resistance. Capacitance was evaluated with a continuous high-resolution, two-sine wave technique fully described elsewhere (15,16). Capacitance data were fitted to the first derivative of a two-state Boltzmann function, to extract Boltzmann parameters (17). A two-state Boltzmann model adequately describes prestin's charge movement (18,19)

$$C_m = Q_{\max}\frac{ze}{kT}\frac{b}{(1+b)^2} + C_{lin}, \qquad (1)$$

where

$$b = \exp\left(\frac{-ze(V_m - V_h)}{kT}\right).$$

$Q_{\max}$ is the maximum nonlinear charge transfer, V_h is the voltage at peak capacitance or half-maximal nonlinear charge transfer, V_m is the membrane potential, C_{lin} is the linear capacitance, z is the unitary charge movement or valence (also a metric of voltage sensitivity), e is the electron charge, k is Boltzmann's constant, and T is the absolute temperature. $Q_{\max}$ is reported as Q_{sp}, the specific charge density, i.e., the total charge moved, normalized to linear capacitance. Student's t-test and analyses of variance (ANOVAs) were used to evaluate the effects of mutations on different parameters of NLC and transport.

RESULTS

Prestin is an anion transporter

Although prestin-induced anion transport is not demonstrable in oocytes, it is possible that transport occurs in other systems. To test whether prestin transports anions in alternative expression systems, we transfected CHO cells with prestin (*Meriones unguiculatus*), and compared anion transport in these cells and in CHO cells transfected with empty vector. As shown in Fig. 1 *A*, CHO cells transfected with prestin showed a time-dependent increase in [^{14}C]formate uptake, compared with cells transfected with vector alone. The CHO cells possess an intrinsic anion-uptake mechanism that accounts for the levels of [^{14}C]formate uptake in cells transfected with empty vector alone. As expected, we also found that the accumulation of [^{14}C]formate was dose-dependent, i.e.,

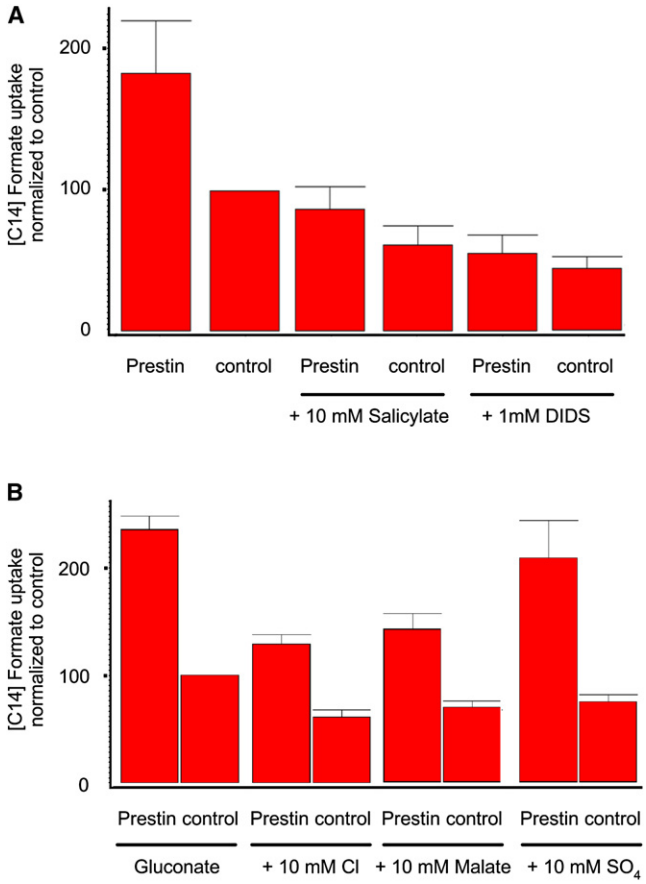

FIGURE 2 Prestin-induced uptake of [^{14}C]formate can be blocked. (*A*) [^{14}C]formate uptake in cells transfected with prestin and vector only, and similarly transfected cells treated with 10 mM salicylate and 1 mM DIDS in incubation/preincubation medium. Prestin-induced uptake of [^{14}C]formate was reduced by both agents. Mean values for the six groups were: prestin, 183 (±37); control, 100, prestin with salicylate, 87 (±16); control with salicylate, 61 (±13.0); prestin with DIDS, 53.9 (± 13.0); and control with DIDS, 44 (±8.5) ($n = 3$). (*B*) Effects of various test anions on prestin-induced uptake of [^{14}C]formate. Prestin-transfected cells were incubated with Na gluconate and Na gluconate to which various indicated test anions were then added. Both chloride and malate decreased prestin uptake, whereas SO_4^{2-} had minimal effects on prestin-induced [^{14}C]formate uptake. Mean values for the eight groups were: prestin, 237 (±11.8); control, 100; prestin + chloride, 130 (±8.6); control + chloride, 61 (±6.7); prestin + malate, 142 (±15); control + malate, 70 (±5.7); prestin + SO_4^{2-}, 209 (±35); and control + SO_4^{2-}, 75 (±6.5). Uptake of [^{14}C]formate by prestin was significantly reduced by chloride and malate ($p < 0.05$, one-way ANOVA), but not by SO_4^{2-} ($p > 0.05$) ($n = 3$). Data were normalized to vector-only controls. Uptake is denoted in relative counts (see Methods).

the amount of prestin plasmid used for transfection correlated with [^{14}C]formate accumulation (Fig. 1 *B*). We then compared the uptake of prestin with SLC26a6, a member of the SLC26 anion transporter family that is most closely related to prestin. As indicated in Fig. 1 *C*, cells transfected with prestin showed a marked increase in [^{14}C]formate uptake that was comparable to that of CHO cells similarly transfected with SLC26a6. The uptake induced by transfected transporters was significantly greater than that for cells transfected with vector only ($p < 0.01$, ANOVA). Fig. 1 *D* summarizes similar positive transport studies with [^{14}C]oxalate. SLC26a6 has a preferred affinity for the oxalate anion, and knockouts of SLC26a6 have defective epithelial Cl-oxalate exchange, leading to oxalate urinary calculi (14,20). The absolute prestin-induced uptake of oxalate was 1.5-fold greater than formate uptake, and is not reflected in the figures, which were normalized to our controls. As noted above, we reinvestigated anion transport in oocytes using [^{14}C]formate and [^{14}C]oxalate uptake, and in contrast to our data with CHO cells, we failed to demonstrate an uptake of these anions by prestin. At best, we found an inconsistent increase in uptake, even when we attempted to maximize translation by using unidirectionally capped cRNA at a concentration of 50 ng per oocyte. These results are consistent with other work in the field, and may result from an absence of an associated cofactor for prestin in oocytes, which is present in CHO cells. Because we lack a quantitative mechanism for determining the expression of prestin on the cell surface, we cannot ascertain if the absence of transport in oocytes results from inadequate surface expression.

Prestin's anion transport is similar to SLC26 family-member anion transporters

The uptake of [^{14}C]formate induced by prestin in CHO cells was blocked by 1 mM 4,4′-diisothiocyanatostilbene-2,2′-disulfonic acid (DIDS), a well-characterized blocker of anion transport (Fig. 2 *A*) (14). Anion transport by other members of the SLC26 anion transporter family was shown to require up to 1 mM DIDS to completely block anion transport. Furthermore, anion transport was also blocked by 10 mM salicylate, which is known to block prestin's NLC (Fig. 2 *A*) (21,22).

After establishing that prestin mediates formate and oxalate transport, we tested the ability of other anions to compete for formate uptake. Anion transporters of the SLC26 family have a variable ability to transport different anions that is, in part, explained by their relative affinity for these anions (23,24). Fig. 2 *B* summarizes experiments where [^{14}C]formate uptake by prestin-transfected CHO cells was measured in the presence of competing extracellular (10 mM) test anions. As is evident, both chloride and malate were able to inhibit the uptake of formate ($p < 0.01$, ANOVA), whereas the divalent anion sulfate had minimal effects on formate uptake ($p > 0.05$, ANOVA). The result with sulfate is interesting, because sulfate was originally thought not to support NLC (8), but was subsequently shown to support robust NLC and electromotility in outer hair cells (9–11,25,26).

Prestin's anion-transporter function can be separated from NLC: the role of a potential chloride-binding site

Chloride plays an important role in generating NLC, whether as its extrinsic voltage sensor or as an intracellular allosteric

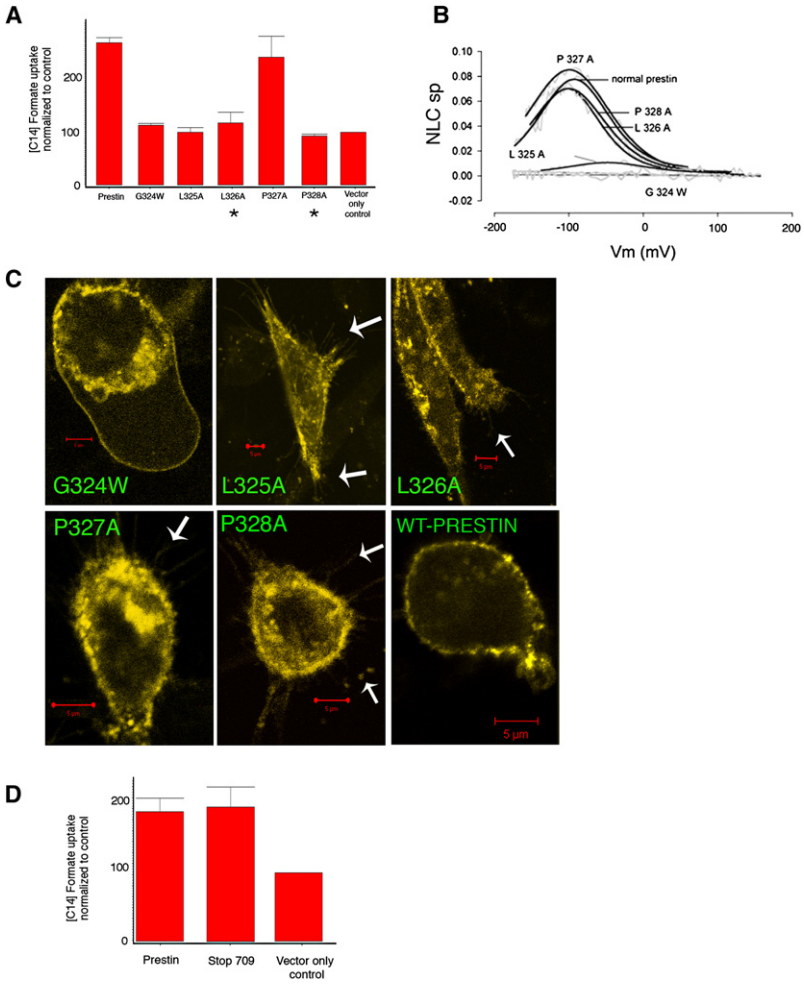

FIGURE 3 Effects of truncations and mutations in prestin on prestin-induced uptake of [^{14}C]formate. (*A*) Single mutations in potential chloride-binding motif decrease anion transport. All mutants except P327A show decreased anion transport. Mean uptake of [^{14}C]formate of prestin, G324W, L325A, L326A, P327A, P328A, and vector-only control cells were 269 (±9), 113 (±3), 100 (±9), 117 (±20), 241 (±40), 93 (±3.5), and 100, respectively. The uptake of [^{14}C]formate by prestin and P327A-transfected cells was significantly greater than in controls ($p < 0.05$, one-way ANOVA) ($n = 4$). (*B*) Effects of these mutations on NLC. Two mutants P328A and L326A show preserved NLC but decreased anion transport (indicated by asterisk in *A*). P327A has preserved NLC and anion transport, whereas remaining mutants eliminated (G324W) or significantly decreased (L325A) NLC, while also decreasing anion transport. (*C*) Confocal microscopy of YFP fusions of prestin and individual mutants (G324W, L325A, L326A, P327A, and P328A) shows membrane targeting. Arrows indicate filopodia containing prestin-YFP fluorescence. (*D*) Truncation of C-terminus at amino acid 709 (stop 709) that eliminates NLC shows preserved anion transport. Mean [^{14}C]formate uptake values for prestin, stop 709, and vector-only control were 188 (±18), 197 (±28), and 100, respectively. The [^{14}C]formate uptakes in prestin and stop 709-transfected cells were significantly greater than in controls ($p < 0.05$) ($n = 3$). Uptake is denoted in relative counts (see Methods).

modulator (8–10). In seeking to understand the action of intracellular chloride, we identified one potential chloride-binding motif in prestin, based on its homology with a proven chloride-binding site (GXXXP) in the bacterial CLC channel (27), where it is thought to bind chloride ions traversing the channel's pore. In prestin, this sequence, GLLPP (amino acids 324–328), lies on the predicted intracellular surface of the protein between transmembrane loops 6 and 7 of the 10-transmembrane model (13). We mutated individual amino acids in this motif, and determined their effects on NLC and anion transport. Four mutations (G324W, L325A, L326A, and P328A) abolished prestin-induced anion transport ($p < 0.01$, one-way ANOVA; Fig. 3 *A*). Correspondingly, one mutation (G324W) abolished NLC, and another (L325A) profoundly reduced NLC, whereas three mutations (L326A, P327A, and P328A) had normal NLC (Fig. 3 *B*). Consequently, two of our mutants (L326A and P328A) exerted differential effects on NLC and anion transport, each preserving the former and reducing the latter. As shown in Fig. 3 *C*, confocal imaging confirmed that all these mutants were targeted to the plasma membrane, even showing an unequivocal fluorescence of filopodia, processes that lack confounding intramembranous organelles. Of course, plasmalemmal targeting was expected for mutations showing NLC, because NLC (or transport) was observed in these mutants, and such functional activity could only have occurred if the proteins were targeted to the membrane where they could sense voltage or mediate the cellular transport of anions.

Although these data clearly show a divorce between transport and NLC, we sought unequivocal corroboration. In previous studies, we and others showed that serial truncations of prestin's C-terminus reduce and then abolish NLC (13,28). Truncation of the C-terminus at amino acid 709 results in a loss of NLC. We tested anion transport (Fig. 3 *D*) in this mutant lacking NLC (stop 709), and found that it had preserved anion transport, equivalent to normal prestin and statistically greater than in cells transfected with control YFP vector alone ($p < 0.05$). We previously demonstrated via confocal microscopy and flow cytometry that this mutant was targeted to the plasma membrane. These transport data confirm the truncation's proper membrane targeting. Clearly, the demonstration of preserved anion transport with this NLC-incompetent mutant confirms that anion transport can be separated from NLC.

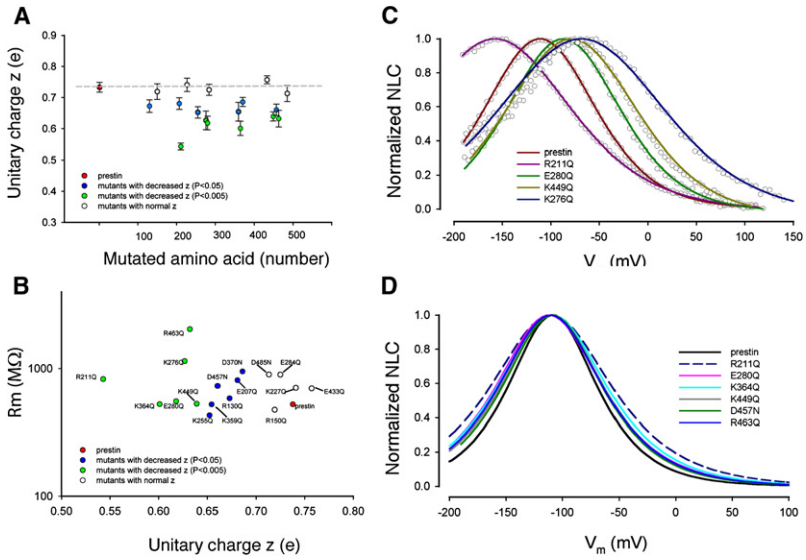

FIGURE 4 Effects of single amino-acid substitutions of charged residues that are within or in close proximity to predicted membrane-spanning regions. (*A*) Effects on unitary charge (z) are shown and plotted against amino-acid position. Data include only those mutants that showed nonlinear capacitance. Residues are grouped according to how significantly different their z values were, compared with wild-type prestin (*red*). Those residues are in blue where $p < 0.05$ (R130Q, R211Q, K255Q, K359Q, D269N, and D457N), and in green where $p < 0.005$ (E207Q, K276Q, E280Q, K364Q, K449Q, and R463Q). (*B*) Average membrane resistance of prestin and prestin mutants in *A*. These data confirm that changes in z were independent of membrane resistance. (*C*) Normalized examples of NLC of prestin and four mutants that showed a reduction in z. Data points are fitted with Eq. 1. (*D*) Normalized average fits of individual mutants are aligned to wild-type prestin's V_h, for a better demonstration of decrease in voltage sensitivity evidenced by a broadening of the functions.

Prestin has an intrinsic voltage sensor

Our results so far provide evidence that key components of the extrinsic voltage-sensor hypothesis (i.e., that transport is absent, along with the reasonable inference that NLC arises from the loss of a full transport cycle) are untenable. Although these results do not disprove the extrinsic-voltage hypothesis, they warrant a reexploration of the model. Moreover, these results beget the question: is there an alternative or additional mechanism whereby prestin senses voltage? We sought to determine if charged residues in prestin's transmembrane domains contribute to its gating charge movement. To do so, we neutralized 22 charged residues that were predicted to lie in its transmembrane regions by site-directed mutagenesis, and determined the effects on the unitary charge movement, z. In contrast to findings by Oliver et al. (8), all these residues were conserved between prestin and its closest relative, SLC26a6. We relied on measures of unitary charge derived from the traditional two-state Boltzmann function as a metric of charge movement within a single motor. It is our best (and only) estimate of charge movement within a single motor. Moreover, empirical data as they relate to prestin function (both charge and electromotility) fit exceedingly well with the two-state Boltzmann function (17–19). Of 22 mutated, charged residues, we found a subset of 12 tat significantly reduced z (Fig. 4 *A* and Table 1). We were careful to exclude potential alterations in membrane resistance characteristics in our evaluations, because membrane resistance remained equivalent to controls (Fig. 4 *B*). The reduced z, evidence of altered voltage-sensing as reflected by reduced voltage sensitivity (i.e., broader NLC functions), is most readily seen in the normalized NLC traces in Fig. 4, *C* and *D*.

In Fig. S1 of the Supporting Material, we show representative C-V functions from all 12 mutants. These 12 residues that affected z are located across the entire span of the transmembrane core of prestin (Fig. 5, *A* and *B*). Of the remaining 10 residues, mutations of five residues failed to affect z (R150, K227, E284, E433, and D485); mutations of four residues (D83, E293, E374, and E404) resulted in absent NLC; and the mutation of one residue (R399) resulted in a V_h shift to an extreme negative range, making the estimation of z impossible. The mutations of the four residues that showed absent NLC were likely attributable to poor membrane-targeting, as evidenced by confocal imaging (data not shown). Of the residues that affected z, four were negatively charged (E207, E280, D370, and D457), and eight residues were positively charged (R130, R211, K255, K276, K359, K364, K449, and R463). The effects on z of all these charged residues varied. These mutations also affected the operating voltage of the protein (V_h), although there was no relationship between z and V_h (Fig. 6). As expected, there was a correlation between z and the total

TABLE 1 *Z* values (±SE) of individual mutations, *p* values of a *t*-test compared with wild-type prestin, and number of cells recorded

Amino acid position	z	p	Number of cells recorded
Wild-type prestin	0.73 ± 0.02		19
R130Q	0.67 ± 0.02	<0.05	11
E207Q	0.68 ± 0.02	<0.05	10
R211Q	0.54 ± 0.01	<0.00000001	15
K255Q	0.65 ± 0.02	<0.01	8
K276Q	0.63 ± 0.03	<0.001	9
E280Q	0.62 ± 0.02	<0.0001	11
K359Q	0.65 ± 0.03	<0.01	11
K364Q	0.60 ± 0.02	<0.0001	9
D370N	0.69 ± 0.01	<0.05	10
K449Q	0.64 ± 0.01	<0.001	10
D457N	0.66 ± 0.02	<0.01	9
R463Q	0.63 ± 0.03	<0.005	9

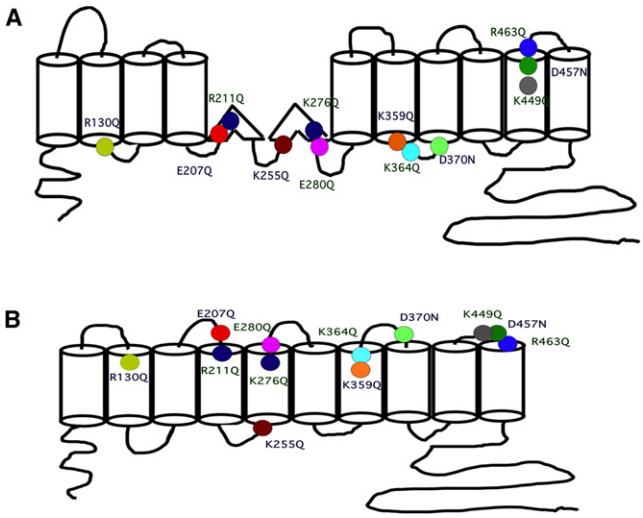

FIGURE 5 Residue locations. Placement of charge residue mutations in 12 (*A*) and 10 (*B*) transmembrane models of the protein. The residues and their traces in Fig. S1 are correspondingly color-coded. Also indicated are specific amino-acid numbers, which in turn are color-coded as in Fig. 4 *A*, to indicate residues and their effects on *z*.

charge movement in prestin and all of its point mutations that affected *z* (Fig. 7).

DISCUSSION

Here we unequivocally showed that prestin, in contrast to our previous understanding, is an anion transporter, much like its closest relative, SLC26a6. Moreover, our results are consistent with the concept of prestin's voltage sensitivity deriving at least in part (and perhaps even entirely) from intrinsic charged residues in the protein. Finally, we were able to separate these two functional characteristics of prestin by mutations to residues within a putative anion-binding site.

The widely accepted notion of an absence of intrinsic voltage-sensing in prestin followed experiments by Oliver et al. (8), who failed to find a change in unitary gating charge after mutating charged residues in prestin that were absent in SLC26a6 (the closest relative that does not exhibit gating charge movement). They reasoned that the gating charge in prestin was attributable to newly acquired charged residues in prestin. In reviewing their mutagenesis experiments, we noted that a significant number (10/21) of charged residues that were different between the two proteins lay outside its predicted transmembrane domain, and therefore could not have sensed transmembrane voltage. Indeed, we mutated charged residues in the intracellular C-terminus, and found that such mutations did not alter the unitary charge relative to controls (29). To test fully for intrinsic voltage-sensing, we mutated every charged residue in prestin that lies within or in very close proximity to the predicted transmembrane segments (of both the 10-transmembrane and 12-transmembrane models; Fig. 5, *A* and *B*), and determined the effect on unitary charge (*z*). We identified a large number of charged residues (12 out of 22)

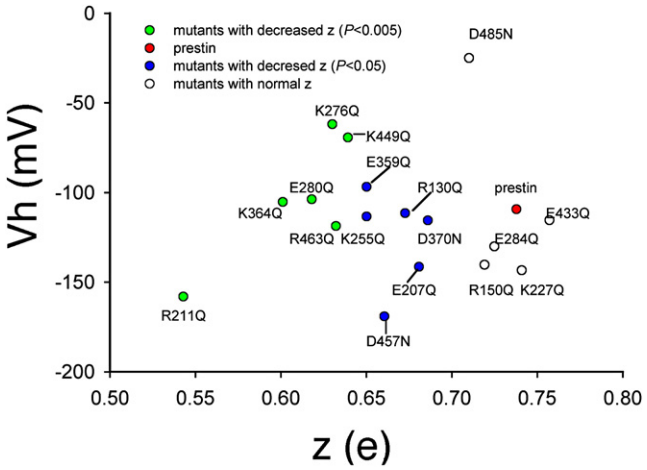

FIGURE 6 Relationship between voltage of peak capacitance (V_h) and unitary charge (*z*). There is no relationship between *z* values and V_h, although most of the mutants caused a negative shift in V_h.

within prestin's transmembrane domains that are also conserved in SLC26a6, and that contribute to the generation of NLC. These data require a fundamental rethinking of how prestin brings about electromotility.

Three features of the identified residues and their relationship to voltage sensitivity are noteworthy. First, prestin shows much less voltage sensitivity than conventional ion channels. Thus, the unitary charge per motor in prestin amounts to ~0.74 e, and contrasts with values of 13.6e for Shaker potassium channels, 10e for sodium channels, and 2.6e for large-conductance, calcium-activated potassium channels (30–33). Second, mutations that produced a reduction in *z*, although they were as low as 0.55, clustered around a mode of 0.65e, indicating that these residues contributed a similar amount of charge to the total gating-charge movement. Third, all of these residues are conserved between prestin and SLC26a6, which does not exhibit gating-charge movement (8) (J.-P. Bai and D. Navaratnam, unpublished observations).

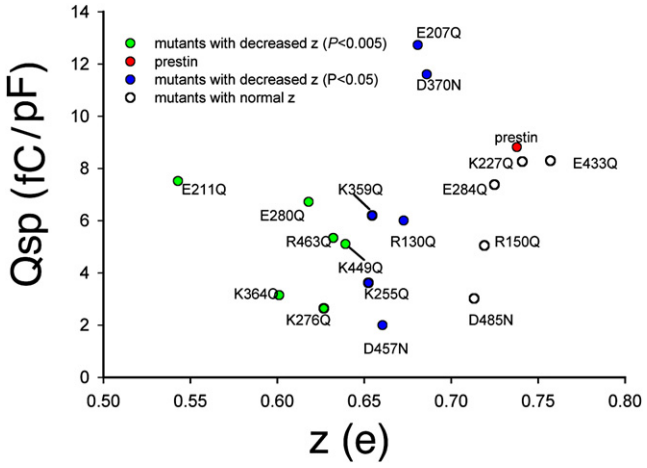

FIGURE 7 Relationship between unitary charge *z* and specific capacitance. There is a positive trend between *z* and Q_{sp} (Q_{max}/linear capacitance).

Why should conserved residues generate a charge movement in one family member but not the other? There are parallels in ion channels where residues that contribute to gating charge and voltage sensitivity in one protein are conserved in a related orthologous protein, yet do not contribute to gating charge or voltage sensitivity in the orthologous protein. For example, the Shab delayed rectifier potassium channel and its mammalian homolog Kv2.1 have the same number of charged residues in their voltage sensors, yet carry different gating charges (7.5e and 12.5e, respectively) (34). Similarly, the gating charge in mSlo channels (2.6e) is fivefold less than that in Shaker channels (13e), although mSlo contains three of the five residues most important for gating charges (33). According to a widely held consensus, these differences are likely attributable to a smaller movement of these residues in both mSlo and Shab (33–35). A similar mechanism could explain the apparent discrepancy between prestin's gating-charge movement and its absence in SLC26a6, which has the same residues implicated in prestin's charge movement. Alternatively, there may be a movement of charged residues of opposite polarity neutralizing their effects in SLC26a6. In any event, the movement of charge through the voltage field in prestin and the contribution from each of these residues to total charge movement are small, when compared with voltage-gated ion channels. In this respect, prestin differs from voltage-gated ion channels, where a few charged residues account for the majority of voltage sensitivity.

Perhaps more germane to the workings of prestin, a member of a transporter family, is the observation that in some transporters, when substrate is removed, presteady-state currents are revealed (36–38). Transient, presteady-state currents are equivalent to the gating-charge movements or NLC measured in prestin, and represent voltage-sensor activity. For example, in line with our determinations for prestin, the voltage-sensing mechanisms in the Na^+-glucose transporter were shown to involve intrinsic charge movements of the protein, rather than only Na^+ binding/unbinding to sites within the protein's membrane field (38,39). Interestingly, the charge valence z of 1e is close to that of prestin. Similarly, it is known that the GABA transporter's charge movement is derived from extrinsic (chloride) and intrinsic charge (36). Indeed, even the chloride dependence of gating in CLC channels is known to arise because of competition with a glutamate gate charge, rather than functioning as a mobile extrinsic voltage sensor (40). Thus, the use of intrinsic charged residues is clearly a general mechanism of voltage-sensing proteins, and prestin is no different (41).

Our data showing separated NLC and anion transport by mammalian prestin contain several implications. First, our data extend work showing that nonmammalian orthologs of prestin are able to transport anions in an electrogenic manner (6). In that study (6), electrophysiological methodology was used solely to assess electrogenic transport, and the authors reasoned that electrogenic transport in mammalian prestin does not occur. Interestingly, however, some electrophysiological characteristics of mammalian prestin were successfully modeled as a result of the exact type of electrogenic transport found in nonmammalian orthologs of prestin (25). Our data cannot resolve this controversy, because the classic transport techniques that we used, although thoroughly sufficient for the demonstration of anion transport, cannot assess electrogenicity. Second, our data suggest that the advent of NLC/electromotility occurs independent of anion transport, and is not coincident with its loss, as previously suggested. Indeed, an evolutionary analysis suggests that SLC26a6, which lacks the ability to generate NLC or electromotility, arose from SLC26a5 (Dr. Kirk Beisel, Creighton University, personal communication, 2008). Third, because each outer hair cell is estimated to contain up to 10 million prestin motors (42,43), our data imply the presence of a powerful homeostatic mechanism for controlling anion concentration in these cells. This is especially the case in light of ample data showing that prestin's operating voltage range is affected by intracellular anion concentration (10,12,44). Fourth, our data showing intrinsic voltage-sensor activity in prestin establish an alternative or additional molecular mechanism for voltage-sensing in the outer hair cell motor. The original extrinsic voltage-sensor or partial anion-transporter model of prestin voltage-sensing, where monovalent chloride anions serve as sources of voltage-sensor charge movement or NLC (8), has received serious challenges. For example, whereas sulfate anions were found to abolish NLC in prestin-transfected cells (8), several groups showed that sulfate supports NLC and electromotility in OHCs (10,11,25,26). Furthermore, anion-charge valence does not dictate gating-charge valence, as would be expected in the extrinsic voltage-sensor model (9). We suggested that anions serve as allosteric modulators, because the conformational state of prestin depends not only on the concentration of intracellular anions, but on their structure as well (9). In this regard, it is interesting that alkylsulfonic anions of differing hydrocarbon chain lengths variably shift prestin's operating voltage range, conceivably because of interactions with the different voltage-sensing residues that we identified here.

Finally, our data raise an important question. Because the advent of the outer hair cell motor is thought to be a recent evolutionary event, and because the residues in prestin responsible for sensing voltage are also present in SLC26a6, what additional features in prestin allow these charged residues to move in response to changes in transmembrane voltage?

SUPPORTING MATERIAL

A figure is available at http://www.biophysj.org/biophysj/supplemental/S0006-3495(09)00470-6.

The authors thank Dr. Fred Sigworth for suggestions, discussions about the data, and critical reading of the manuscript.

Support was provided by National Institutes of Health National Institute on Deafness and Other Communication Disorders grants DC 000273 (to J.S.S.) and DC 008130 (to J.S.S. and D.N.).

REFERENCES

1. Zheng, J., W. Shen, D. He, K. Long, L. Madison, et al. 2000. Prestin is the motor protein of cochlear outer hair cells. *Nature*. 405:149–155.
2. Santos-Sacchi, J., W. X. Shen, J. Zheng, and P. Dallos. 2001. Effects of membrane potential and tension on prestin, the outer hair cell lateral membrane motor protein. *J. Physiol. (Lond.)*. 531:661–666.
3. Ludwig, J., D. Oliver, G. Frank, N. Klocker, A. W. Gummer, et al. 2001. Reciprocal electromechanical properties of rat prestin: the motor molecule from rat outer hair cells. *Proc. Natl. Acad. Sci. USA*. 98:4178–4183.
4. Liberman, M. C., J. Gao, D. Z. He, X. Wu, S. Jia, et al. 2002. Prestin is required for electromotility of the outer hair cell and for the cochlear amplifier. *Nature*. 419:300–304.
5. Reference deleted in proof.
6. Schaechinger, T. J., and D. Oliver. 2007. Nonmammalian orthologs of prestin (SLC26A5) are electrogenic divalent/chloride anion exchangers. *Proc. Natl. Acad. Sci. USA*. 104:7693–7698.
7. Dallos, P., and B. Fakler. 2002. Prestin, a new type of motor protein. *Nat. Rev. Mol. Cell Biol.* 3:104–111.
8. Oliver, D., D. Z. He, N. Klocker, J. Ludwig, U. Schulte, et al. 2001. Intracellular anions as the voltage sensor of prestin, the outer hair cell motor protein. *Science*. 292:2340–2343.
9. Rybalchenko, V., and J. Santos-Sacchi. 2008. Anion control of voltage sensing by the motor protein prestin in outer hair cells. *Biophys. J.* 95:4439–4447.
10. Rybalchenko, V., and J. Santos-Sacchi. 2003. Cl^- flux through a non-selective, stretch-sensitive conductance influences the outer hair cell motor of the guinea-pig. *J. Physiol.* 547:873–891.
11. Rybalchenko, V., and J. Santos-Sacchi. 2003. Allosteric modulation of the outer hair cell motor protein prestin by chloride. *In* Biophysics of the Cochlea: From Molecules to Models. A. Gummer, editor. World Scientific Publishing, Singapore. 116–126.
12. Song, L., A. Seeger, and J. Santos-Sacchi. 2005. On membrane motor activity and chloride flux in the outer hair cell: lessons learned from the environmental toxin tributyltin. *Biophys. J.* 88:2350–2362.
13. Navaratnam, D., J. P. Bai, H. Samaranayake, and J. Santos-Sacchi. 2005. N-terminal-mediated homomultimerization of prestin, the outer hair cell motor protein. *Biophys. J.* 89:3345–3352.
14. Jiang, Z., I. I. Grichtchenko, W. F. Boron, and P. S. Aronson. 2002. Specificity of anion exchange mediated by mouse Slc26a6. *J. Biol. Chem.* 277:33963–33967.
15. Santos-Sacchi, J. 2004. Determination of cell capacitance using the exact empirical solution of dY/dCm and its phase angle. *Biophys. J.* 87:714–727.
16. Santos-Sacchi, J., S. Kakehata, and S. Takahashi. 1998. Effects of membrane potential on the voltage dependence of motility-related charge in outer hair cells of the guinea-pig. *J. Physiol.* 510:225–235.
17. Santos-Sacchi, J. 1991. Reversible inhibition of voltage-dependent outer hair cell motility and capacitance. *J. Neurosci.* 11:3096–3110.
18. Santos-Sacchi, J. 1993. Harmonics of outer hair cell motility. *Biophys. J.* 65:2217–2227.
19. Scherer, M. P., and A. W. Gummer. 2005. How many states can the motor molecule, prestin, assume in an electric field? *Biophys. J.* 88:L27–L29.
20. Jiang, Z., J. R. Asplin, A. P. Evan, V. M. Rajendran, H. Velazquez, et al. 2006. Calcium oxalate urolithiasis in mice lacking anion transporter Slc26a6. *Nat. Genet.* 38:474–478.
21. Tunstall, M. J., J. E. Gale, and J. F. Ashmore. 1995. Action of salicylate on membrane capacitance of outer hair cells from the guinea-pig cochlea. *J. Physiol.* 485:739–752.
22. Kakehata, S., and J. Santos-Sacchi. 1996. Effects of salicylate and lanthanides on outer hair cell motility and associated gating charge. *J. Neurosci.* 16:4881–4889.
23. Markovich, D., and P. S. Aronson. 2006. Specificity and regulation of renal sulfate transporters. *Annu. Rev. Physiol.* 69:361–375.
24. Mount, D. B., and M. F. Romero. 2004. The SLC26 gene family of multifunctional anion exchangers. *Pflugers Arch.* 447:710–721.
25. Muallem, D., and J. Ashmore. 2006. An anion antiporter model of prestin, the outer hair cell motor protein. *Biophys. J.* 90:4035–4045.
26. Kennedy, H. J., M. G. Evans, A. C. Crawford, and R. Fettiplace. 2006. Depolarization of cochlear outer hair cells evokes active hair bundle motion by two mechanisms. *J. Neurosci.* 26:2757–2766.
27. Estevez, R., and T. J. Jentsch. 2002. CLC chloride channels: correlating structure with function. *Curr. Opin. Struct. Biol.* 12:531–539.
28. Zheng, J., G. G. Du, K. Matsuda, A. Orem, S. Aguinaga, et al. 2005. The C-terminus of prestin influences nonlinear capacitance and plasma membrane targeting. *J. Cell Sci.* 118:2987–2996.
29. Bai, J. P., D. Navaratnam, H. Samaranayake, and J. Santos-Sacchi. 2006. En bloc C-terminal charge cluster reversals in prestin (SLC26A5): effects on voltage-dependent electromechanical activity. *Neurosci. Lett.* 404: 270–275.
30. Aggarwal, S. K., and R. MacKinnon. 1996. Contribution of the S4 segment to gating charge in the Shaker K^+ channel. *Neuron*. 16:1169–1177.
31. Seoh, S. A., D. Sigg, D. M. Papazian, and F. Bezanilla. 1996. Voltage-sensing residues in the S2 and S4 segments of the Shaker K^+ channel. *Neuron*. 16:1159–1167.
32. Yang, N., A. L. George, Jr., and R. Horn. 1996. Molecular basis of charge movement in voltage-gated sodium channels. *Neuron*. 16:113–122.
33. Horrigan, F. T., J. Cui, and R. W. Aldrich. 1999. Allosteric voltage gating of potassium channels I. Mslo ionic currents in the absence of Ca(2+). *J. Gen. Physiol.* 114:277–304.
34. Islas, L. D., and F. J. Sigworth. 1999. Voltage sensitivity and gating charge in Shaker and Shab family potassium channels. *J. Gen. Physiol.* 114:723–742.
35. Ma, Z. M., X. J. Lou, and F. T. Horrigan. 2006. Role of charged residues in the S1–S4 voltage sensor of BK channels. *J. Gen. Physiol.* 127:309–328.
36. Sacher, A., N. Nelson, J. T. Ogi, E. M. Wright, D. D. Loo, et al. 2002. Presteady-state and steady-state kinetics and turnover rate of the mouse gamma-aminobutyric acid transporter (mGAT3). *J. Membr. Biol.* 190:57–73.
37. Hazama, A., D. D. Loo, and E. M. Wright. 1997. Presteady-state currents of the rabbit Na^+/glucose cotransporter (SGLT1). *J. Membr. Biol.* 155:175–186.
38. Loo, D. D., B. A. Hirayama, A. Cha, F. Bezanilla, and E. M. Wright. 2005. Perturbation analysis of the voltage-sensitive conformational changes of the Na^+/glucose cotransporter. *J. Gen. Physiol.* 125:13–36.
39. Aronson, P. S. 1978. Energy-dependence of phlorizin binding to isolated renal microvillus membranes. Evidence concerning the mechanism of coupling between the electrochemical Na^+ gradient the sugar transport. *J. Membr. Biol.* 42:81–98.
40. Dutzler, R., E. B. Campbell, and R. MacKinnon. 2003. Gating the selectivity filter in ClC chloride channels. *Science*. 300:108–112.
41. Bezanilla, F. 2008. How membrane proteins sense voltage. *Nat. Rev. Mol. Cell Biol.* 9:323–332.
42. Huang, G. J., and J. Santos-Sacchi. 1993. Mapping the distribution of the outer hair cell motility voltage sensor by electrical amputation. *Biophys. J.* 65:2228–2236.
43. Gale, J. E., and J. F. Ashmore. 1997. The outer hair cell motor in membrane patches. *Pflugers Arch.* 434:267–271.
44. Santos-Sacchi, J., L. Song, J. Zheng, and A. L. Nuttall. 2006. Control of mammalian cochlear amplification by chloride anions. *J. Neurosci.* 26:3992–3998.